Lasing characteristics of strongly pumped Yb-doped photonic crystal fiber laser

Kang Li (李 康)[1,2], Yishan Wang (王屹山)[1], Wei Zhao (赵 卫)[1], Guofu Chen (陈国夫)[1], Qinjun Peng (彭钦军)[3], Dafu Cui (崔大复)[3], and Zuyan Xu (许祖彦)[3]

[1]*State Key Laboratory of Transient Optics & Photonics, Xi'an Institute of Optics & Precision Mechanics, Chinese Academy of Sciences, Xi'an 710068*

[2]*Graduate School of the Chinese Academy of Sciences, Beijing 100039*

[3]*Key Laboratory of Optical Physics, Institute of Physics, Chinese Academy of Sciences, Beijing 100080*

Received November 10, 2006

A strongly pumped Yb-doped large-mode-area photonic crystal fiber (LMA-PCF) laser is analyzed. The lasing characteristics of an improved Fabry-Perot (F-P) cavity fiber laser using LMA-PCF are studied theoretically based on a rate equation model and the exact numerical solution of the rate equations is in excellent agreement with the experimental result.

OCIS codes: 140.3480, 140.3510, 060.2430.

Strongly pumped fiber lasers with highly bright beam output impose a number of requirement on double-clad fiber with the properties of single mode, large mode areas, and large pump cladding with large numerical aperture (NA) which have difficulties in standard fiber technology. Photonic crystal fiber (PCF) represents a technology to solve these problems. Recently even an Yb-doped double-clad PCF with a core diameter of 60 μm and mode-field-area (MFA) of $\sim$ 2000 μm^2 of the emitted fundamental mode has been reported[1]. With the development of PCF technology, high power fiber lasers based on Yb-doped large-mode-area PCF (LMA-PCF) have been the focus of considerable researches[2−5]. Output power up to 1.53 kW of the fiber laser based on LMA-PCF has been obtained[5], which can be compared with the 1.36-kW output power of the fiber laser based on conventional Yb-doped double-clad fibers[6]. Previously published works about the high power LMA-PCF laser concentrate mostly on the experimental studies[2−4]. Some other studies of modeling fiber lasers are interested in the low-power fiber lasers which ignore scattering losses or the effect of laser parameters[7−10]. As for a modeling of strongly pumped fiber laser, Kelson *et al.*[11,12] have studied the approximate analytical and quasi analytical expressions of the rate equations with some assumptions, which cannot analyze the characteristics of inner cavity such as the gain and power distribution along the fiber. Moreover, few studies are involved with the modeling of the strongly pumped fiber laser based on LMA-PCF.

In this letter, we study the lasing characteristics of strongly pumped Yb-doped LMA-PCF laser using a rate equation model in which polarization effects and interactions between neighboring ions are ignored. Using LMA-PCF in this model we find that the exact numerical solutions of a set of coupled differential equations are in excellent agreement with the experimental data.

Yb-doped LMA-PCFs provided by crystal fiber A/S was used in our model and experiments. For the fiber of LMA-PCF-40, the Yb-doped core is formed by seven missing air holes resulting in a hexagonal shaped core and has a diameter of 40 μm as shown in Fig. 1(a). The core is surrounded by four rings of air holes, d is about 1.1 μm and Λ is 12.3 μm ($d/\Lambda = 0.09$). The effective core NA is 0.03 at 1060 nm and the fundamental mode field diameter (MFD) is about 35 μm (MFA $\sim$ 1000 μm^2). The V parameter for a PCF is given by Ref. [13], $V_{\rm PCF} = 2\pi\frac{\Lambda}{\lambda}{\rm NA}(\lambda)$, where NA($\lambda$) is NA of the wavelength dependent effective core of the fundamental mode. Therefore, using the LMA-PCF parameters stated above we can calculate the $V_{\rm PCF}$ parameter approximately.

A typical fiber laser with single-end cladding-pump which does not include pump power reflection is illustrated in Fig. 2. For continuous wave (CW) lasers, the time-independent steady-state rate equations are given

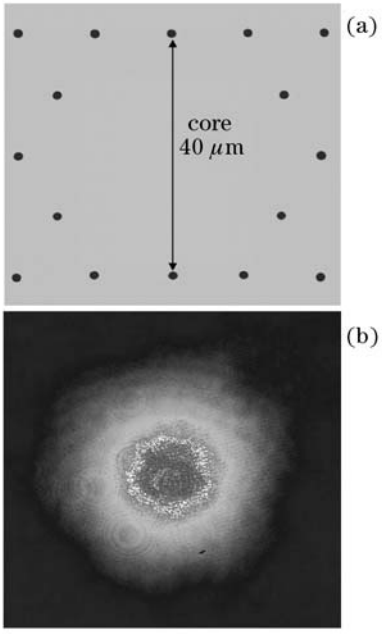

Fig. 1. (a) Scanning electron micrographs of the core area of LMA-PCF-40; (b) measured intensity distribution of the emitted beam of fiber laser with the fiber of LMA-PCF-40.

by Ref. [11]. The propagation of the pump and signal intensities in the LMA-PCF can be described by the following set of coupled differential equations:

$$\frac{N_2(z)}{N}=\frac{\frac{\left(P_{\rm p}^{+}(z)+P_{\rm p}^{-}(z)\right)\sigma_{\rm a}(\lambda_{\rm p})\Gamma_{\rm p}}{h\nu_{\rm p}A}+\frac{\Gamma_{\rm s}\sigma_{\rm a}(\lambda_{\rm s})}{h\nu_{\rm s}A}\left(P_{\rm s}^{+}(z)+P_{\rm s}^{-}(z)\right)}{\frac{\left(P_{\rm p}^{+}(z)+P_{\rm p}^{-}(z)\right)(\sigma_{\rm a}(\lambda_{\rm p})+\sigma_{\rm e}(\lambda_{\rm p}))\Gamma_{\rm p}}{h\nu_{\rm p}A}+\frac{1}{\tau}+\frac{\Gamma_{\rm s}(\sigma_{\rm a}(\lambda_{\rm s})+\sigma_{\rm e}(\lambda_{\rm s}))}{h\nu_{\rm s}A}\left(P_{\rm s}^{+}(z)+P_{\rm s}^{-}(z)\right)},\tag{1}$$

$$\pm\frac{{\rm d}P_{\rm p}^{\pm}(z)}{{\rm d}z}=-\Gamma_{\rm p}\left[\sigma_{\rm a}(\lambda_{\rm p})N-\left(\sigma_{\rm a}(\lambda_{\rm p})+\sigma_{\rm e}(\lambda_{\rm p})\right)N_2(z)\right]P_{\rm p}^{\pm}(z)-\alpha_{\rm p}P_{\rm p}^{\pm}(z),\tag{2}$$

$$\pm\frac{{\rm d}P_{\rm s}^{\pm}(z)}{{\rm d}z}=\Gamma_{\rm s}\left[\left(\sigma_{\rm a}(\lambda_{\rm s})+\sigma_{\rm e}(\lambda_{\rm s})\right)N_2(z)-\sigma_a(\lambda_{\rm s})N\right]P_{\rm s}^{\pm}(z)+\Gamma_{\rm s}\sigma_{\rm e}(\lambda_{\rm s})N_2(z)P_0(\lambda_{\rm s})-\alpha_{\rm s}P_{\rm s}^{\pm}(z),\tag{3}$$

$P_{\rm p}^{\pm}(z)$ and $P_{\rm s}^{\pm}(z)$ are the pump and signal powers, respectively, propagating in the fiber. The plus and minus superscripts represent propagation along the positive and negative z-directions, respectively, the p and s superscripts represent pump and signal lights, respectively. In our model, we do not consider $P_{\rm p}^{-}(z)$ because the positive pump power is absorbed almost entirely then pump power reflections are ignored. A is the cross-section area of the core and the positive coefficients $\alpha_{\rm s}$ and $\alpha_{\rm p}$ represent the scattering losses for the signal and pump, respectively. The upper lasing level population density is given by $N_2(z)$ with spontaneous lifetime of τ and $N=N_1(z)+N_2(z)$ is the concentration density of Yb ions, $\nu_{\rm p}$ and $\nu_{\rm s}$ are the pump and signal frequencies, respectively. $P_0(\lambda_{\rm s})=2hc^2/\lambda_{\rm s}^3$ represents the contribution of the spontaneous emission into the propagating laser mode. $\sigma_{\rm a}(\lambda)$ and $\sigma_{\rm e}(\lambda)$ are the absorption and emission cross section, respectively. The rate equations are to be solved subject under the boundary conditions:

$$P_{\rm s}^{+}(0)=R_{\rm s}(0)P_{\rm s}^{-}(0),\quad P_{\rm s}^{-}(L)=R_{\rm s}(L)P_{\rm s}^{+}(L),\tag{4}$$

where $R_{\rm s}(0)$ and $R_{\rm s}(L)$ are the effective reflectivities of signal lights at $Z=0$ and $Z=L$, respectively.

In our rate equations, we include amplified spontaneous emission (ASE) and consider scattering losses both for the signal and pump light. However, we ignore nonlinear effects such as dipole-dipole interaction, clustering, and quenching which are significant only in much higher dopant concentrations[14]. As already stated, it is convenient to make use of double-clad fibers with a very large multimode pump cladding area S and NA in order to achieve a good coupling efficiency of pump power. This means that the V parameter for the beam propagating in the multimode pump cladding is very large. For $V\geq 20$ the pump intensity distribution can be assumed constant in the pump cladding[15]. As for LMA-PCF-40, the pump power filling factor which means the fraction of the pump power actually coupled to the active core can be given by the simple expression of $\Gamma_{\rm p}\cong A/S$. The fraction of the signal amplified in the core is described by the signal power filling factors $\Gamma_{\rm s}$. The core areas of LMA-PCF-40 do not have the circular cross section strictly and the experimental laser beam profiles shown in Fig. 1(b) exhibit the hexagonal shape respectively, however, the center part of beam profiles, where most of the power is located, possesses a nearly round and Gaussian like intensity distribution. In order to obtain the suitable value of $\Gamma_{\rm s}$ in LMA-PCF-40 we use an approximation of circular cross section for core area of the two fibers in the weakly waveguide. Using the crucial parameter $V_{\rm PCF}$ and the approximation defined above we can give the value of $\Gamma_{\rm s}$ for the lowest order $\rm LP_{01}$ mode of LMA-PCF laser by Ref. [16].

In our experiment configuration shown in Fig. 3, a dichotic mirror having high transmission of 95% at the pump wavelength (970—980 nm) and high reflectivity R_1 of 99.5% at the signal wavelength (1020—1080 nm) are placed into the coupler directly. Moreover, the dichroic mirror can be adjusted conveniently and does not make an impact on the coupling of the pump lights. The laser output coupler is formed by dichroic mirrors with reflectivity R_2 at the signal wavelength (1020—1080 nm), such as 4%, 10%, 20% and 40%, instead of 4% Fresnel reflections which have the strict requirement for the planeness of the fiber end facet. Both end sections of LMA-PCF-40 are sealed by thermally collapsing the cladding holes over about 400-μm-long section starting from each fiber end. The sealed regions act as nonguiding endcaps in which the beam can freely expand before reaching the silica-air interface, which prevents facet damages. A $\sim 6^\circ$ angle polish is performed to reduce the pump reflection back to the pump power source at the fiber facet, and to avoid the 4% Fresnel reflections which will bring compound cavity in the fiber laser system. In order to observe the mode field characteristics, the output beam is finally detected with a charge coupled device (CCD) camera connected to a mode profiling system.

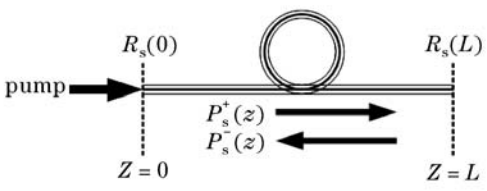

Fig. 2. Schematic of the single-end cladding-pump fiber laser without pump power reflection.

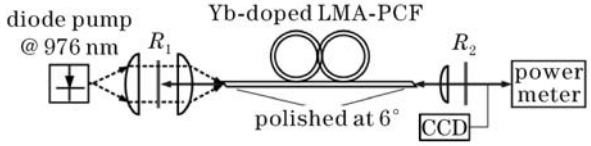

Fig. 3. Scheme of the experimental setup, R_1 and R_2 are the reflectivities of high reflection dichotic mirror and output coupling dichroic mirror at the signal wavelength, respectively.

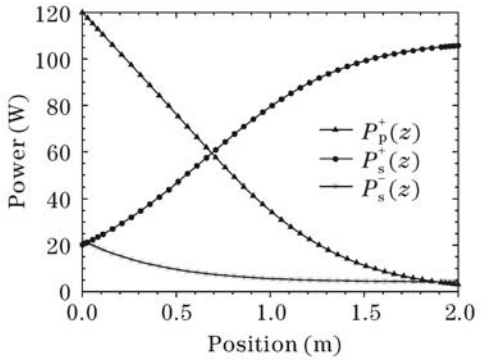

Fig. 4. Calculated distribution of pump and signal power along the fiber of LMA-PCF-40.

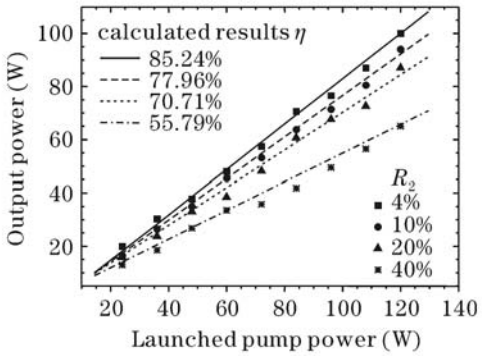

Fig. 5. Output power of the fiber laser with the fiber of LMA-PCF-40 as a function of the launched pump power.

Table 1. Parameters for Numerical Analysis

Yb^{3+} Parameter		Fiber Parameter	
λ_p	976 nm	LMA-PCF-40	
λ_s	1060 nm	A	12.5×10^{-10} m^2
τ	0.84	N	5×10^{25} m^{-3}
σ_{ap}	2.6×10^{-24} m^2	α_p	0.005 m^{-1}
σ_{ep}	2.6×10^{-24} m^2	α_s	0.005 m^{-1}
σ_a (λ_s)	2.6×10^{-25} m^2	Γ_p	0.0440
σ_e (λ_s)	6×10^{-27} m^2	Γ_s	0.7851
h	6.626×10^{-34}	L	2 m

The variations of pump and signal light power along LMA-PCFs without pump reflections, which are calculated from Eqs. (1)—(4), are shown in Fig. 4. The value of $R_s(0)$ and $R_s(L)$ are 95% and 3.8%, respectively. Table 1 shows the parameters used for the rate equation model. As we can see from Fig. 4, laser power densities grow rapidly at first 1.5 meters in LMA-PCF-40 as a result of the strong pump absorption along fiber near the pumping end then trend to gentleness. We can easily calculate the laser output power and slope efficiency by

$$P_{out} = (1 - R_s(L))P_s^+(L), \tag{5}$$

$$\eta = P_{out}/P_p, \tag{6}$$

where P_p is the launched pump power. In Fig. 4, 2-m-long LMA-PCF-40 is used and the calculated output power is about 105 W at a launched pump power of 120 W.

Figure 5 shows the P_{out} of the fiber laser based on LMA-PCF-40 as a function of launched pump power P_p. The values of P_p are measured by cutting back method in our experiments. The solid lines calculated from Eqs. (1)—(6) in Fig. 5 represent the variation of P_{out} as a function of P_p with $R_s(0)$ of 96% and different $R_s(L)$. We need to point out that the value of $R_s(L)$ used in our model is about 95% of the value of R_2 for the feedback signal light loss in transmission through the coupling lens. While the dichroic mirrors with R_2 of 4%, 10%, 20%, and 40% are used, the values of $R_s(L)$ used are about 3.8%, 9.5%, 19%, and 38%, then the calculated values of η are about 85.24%, 77.96%, 70.71%, and 55.79%, respectively. In Fig. 6, we show the variation of

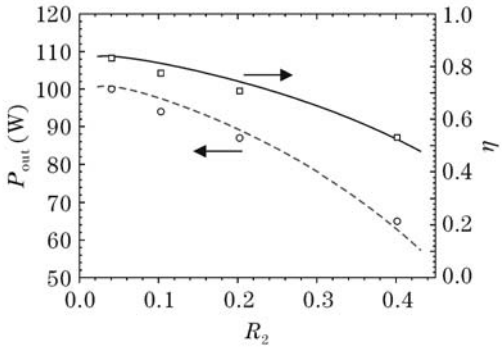

Fig. 6. Output power P_{out} and slope efficiency η as functions of R_2 in the fiber laser with the fiber of LMA-PCF-40 at the launched pump power of 120 W.

P_{out} and η as a function of R_2 in the fiber laser with the fiber of LMA-PCF-40, where the value of R_1 is 99.5% and the launched pump power is 120 W. While we use the dichroic mirrors with different values of R_2 in the experiments, the values of P_{out} and η are obtained and shown to be in excellent agreement with the calculated results from Eqs. (1)—(6). Moreover, 103-W single fundamental mode CW output power with a slope efficiency η of 83.2% is achieved when the whole pump power is up to 210 W with $R_2$of 4%, and the corresponding optical-to-optical conversion efficiency is more than 49%.

In conclusion, we studied the lasing characteristics of a strongly pumped Yb-doped LMA-PCF laser with an improved F-P cavity using a rate equation model. Some effects of dipole-dipole interaction, clustering, quenching, and Rayleigh back scattering are ignored and an approximation of circular cross section for the core area of LMA-PCF in the weakly waveguide is used to introduce some parameters in our model. The exact numerical solutions of Eqs. (1)—(6) are shown to be in excellent coincident with the experimental data. Furthermore, 103-W single fundamental mode CW output power with a slope efficiency of 83.2% is obtained based on LMA-PCF-40, and we find the lengths of LMA-PCF in our experiments are not long enough to absorb the pump lights, which has been predicted in our model.

This work was supported by the National Natural Science Foundation of China under Grant No. 60537060 and 10390160. K. Li's e-mail address is likang@opt.ac.cn.

References

1. J. Limpert, O. Schmidt, J. Rothhardt, F. Röser, T. Schreiber, A. Tünnermann, S. Ermeneux, P. Yvernault, and F. Salin, Opt. Express **14,** 2715 (2006).
2. K. Furusawa, A. Malinowski, J. H. V. Price, T. M. Monro, J. K. Sahu, J. Nilsson, and D. J. Richardson, Opt. Express **9,** 714 (2001).
3. W. J. Wadsworth, R. M. Percival, G. Bouwmans, J. C. Knight, and P. St. J. Russell, Opt. Express **11,** 48 (2003).
4. J. Limpert, T. Schreiber, S. Nolte, H. Zellmer, A. Tünnermann, R. Iliew, F. Lederer, J. Broeng, G. Vienne, A. Petersson, and C. Jakobsen, Opt. Express **11,** 818 (2003).
5. G. Bonati, H. Voelckel, T. Gabler, U. Krause, A. Tünnermann, J. Limpert, A. Liem, T. Schreiber, S. Nolte, and H. Zellmer, Late Breaking News, Photonics West, San Jose, CA, 2005.
6. Y. Jeong, J. K. Sahu, D. N. Payne, and J. Nilsson, Opt. Express **12,** 6088 (2004).
7. M. J. F. Digonnet, K. Liu, and H. J. Shaw, IEEE J. Quantum Electron. **26,** 1105 (1990).
8. F. Sanchez, B. Meziane, T. Chartier, G. Stephan, and P. L. Francois, Appl. Opt. **34,** 7674 (1995).
9. Th. Pfeiffer, H. Schmuck, and H. Bulow, IEEE Photon. Technol. Lett. **4,** 847 (1992).
10. C. Barnard, P. Myslinsky, J. Chrostowsky, and M. Kavehrad, IEEE J. Quantum Electron. **30,** 1817 (1994).
11. I. Kelson and A. A. Hardy, IEEE J. Quantum Electron. **34,** 1570 (1998).
12. I. Kelson and A. Hardy, J. Lightwave Technol. **17,** 891 (1999).
13. N. A. Mortensen, J. R. Folkenberg, M. D. Nielsen, and K. P. Hansen, Opt. Lett. **28,** 1879 (2003).
14. E. Delevaque, T. Georges, M. Monerie, P. Lamouler, and J. F. Bayon, IEEE Photon. Technol. Lett. **5,** 73 (1993).
15. A. Bertoni and G. C. Reali, Appl. Phys. B **66,** 547 (1998).
16. A. W. Snyder and J. D. Love, *Optical Waveguide Theory* (Chapman and Hall, New York, 1983).